Applied Surface Science 282 (2013) 838–843

Contents lists available at SciVerse ScienceDirect

Applied Surface Science

journal homepage: www.elsevier.com/locate/apsusc

# Physical activation of diatomite-templated carbons and its effect on the adsorption of methylene blue (MB)

Dong Liu[a], Weiwei Yuan[a,b], Peng Yuan[a,*], Wenbin Yu[a,b], Daoyong Tan[a,b], Hongmei Liu[a,b], Hongping He[a]

[a] CAS Key Laboratory of Mineralogy and Metallogeny, Guangzhou Institute of Geochemistry, Chinese Academy of Sciences, Guangzhou 510640, China
[b] University of Chinese Academy of Sciences, Beijing 100049, China

ARTICLE INFO

*Article history:*
Received 2 May 2013
Received in revised form 9 June 2013
Accepted 13 June 2013
Available online 25 June 2013

*Keywords:*
Diatomite-templated carbon
Physical activation methods
$CO_2$ activation
$H_2O$ activation
Porosity enhancement
Methylene blue adsorption

ABSTRACT

One- and two-step physical activation methods, using $CO_2$ and $H_2O$ as activation agents, were performed to enhance the porosity of diatomite-templated carbons. The morphology, pore parameters, and adsorption capacity of diatomite-templated carbons before and after activation were investigated to evaluate the effects of activation. The results showed deconstruction of the macroporous structure occurred after one-step activation, while two-step activation retained the unique tubular and pillared macroporous structure of diatomite-templated carbon, indicating a highly promising activation method. The new-appearing pores after two-step activation were mainly micropores, which formed on the walls of carbon tubes and pillars. Pore parameters, such as the specific surface area and pore volume, as well as the micropore volume, showed a great increase after two-step activation and were 2–3 times larger than those of the original carbon. $CO_2$ was more effective in enhancing the porosity than $H_2O$ during two-step activation, and the obtained carbon products had a higher specific surface area and pore volume. Moreover, the carbon products after two-step activation possessed a larger adsorption capacity of methylene blue than the original carbon; the maximum Langmuir adsorption capacity of MB on the $CO_2$-activated carbon was 505.1 mg/g.



## 1. Introduction

Porous carbons are used extensively in gas separation, water purification, catalytic reactions, and electrochemical processing, due to their high specific surface area ($S_{BET}$), large pore volume ($V_p$), chemical inertness, and good mechanical and thermal stability [1,2]. The templating method, one of the well-established processes, has been widely used to synthesize porous carbons with a pore structure that can be controlled by selecting and adjusting the template [3–5]. Zeolite [6–8], silica-mesoporous materials [3,9], and diatomite [10–13] have been used as templates to prepare carbons containing predominantly micropores, mesopores, or macropores, respectively. Among them, preparation of diatomite-templated carbons has attracted increasing attention because the resulting carbon has unique developed macropores and exhibits promising applications in the adsorption and support of large molecules.

Diatomite (diatomaceous earth), a natural biogenetic mineral, is mainly composed of amorphous silica, which was sourced from diatom shells and classified as non-crystalline opal-A in mineralogy [14]. Diatom shells are rich with macropores that have sizes extending from the nanometric to the micrometric domain, as well as containing a few mesopores and micropores. Accordingly, diatomite has been used as the adsorbent, the support, and the template of macroporous materials [15–20]. Macroporous diatomite-templated carbons were first prepared by Holmes et al. [13] and Cai et al. [21], using the sucrose as the carbon source and sulfuric acid as the catalyst for the polymerization of the sucrose. The derived carbon was of developed the porosity, composed of micropores and macropores resulting from the carbonization of sucrose and replication of diatomite macropores, respectively. Subsequently, Perez-Cabero and co-workers introduced $AlCl_3$ as the solid acid catalyst of the carbon precursor on the surface of a cultured diatom and prepared diatom shell-templated carbons [12]. In our previous studies, furfuryl alcohol, the carbon source, was found to be catalyzed by the inherent solid acid sites of diatomite, and thus the

* Corresponding author at: Guangzhou Institute of Geochemistry, Chinese Academy of Sciences, Wushan, Guangzhou 510640, China. Tel.: +86 20 85290341; fax: +86 20 85290341.
*E-mail address:* yuanpeng@gig.ac.cn (P. Yuan).

0169-4332/$ – see front matter © 2013 Elsevier B.V. All rights reserved.
http://dx.doi.org/10.1016/j.apsusc.2013.06.067

diatomite-templated carbon was synthesized without any additive catalyst [10,11]. The derived carbons contained a hierarchically porous structure. This porous structure included micropores, mesopores, and macropores, which were resulted from, respectively, the break of the carbon film, the stacking of carbon particles, and the replication of diatomite macropores. The macroporous structure was composed of carbon tubes and pillars. The tubes were completely hollow, which were derived from the replication of the edge macropores of the diatom shell, and had diameters of 80–200 nm. The pillars derived from the central pores of the diatom shell were mostly solid with hollow ends and had diameters of 250–750 nm [10].

However, these templated carbons obtained with or without an additional acid catalyst do not have notably high $S_{BET}$ (maximum: 426 $m^2/g$) and $V_p$ values (maximum: 0.470 $cm^3/g$)—especially micropore volumes ($V_m$ maximum: 0.195 $cm^3/g$) [11]. And thus, although the carbons possessed a hierarchically porous structure, diatomite-templated carbons showed a low adsorption capacity; for example, the maximum Langmuir adsorption capacity for methylene blue (MB) was only 333.3 mg/g [11], which was smaller than that of industrial activated carbons [22,23]. Therefore, it is necessary to enhance the porosity of diatomite-templated carbons.

Physical activation methods are often used to enhance the porosity during the preparation of activated carbons (micropore-predominant carbons), and $CO_2$ and $H_2O$ are the usual activation agents [24]. An abundance of pores, particular micropores, were generated after activation due to the oxidation of partial carbon atoms by $CO_2$ or $H_2O$. Two well-established activation methods, namely the two-step procedure and the one-step procedure, have been performed. For the former, the route involves carbonization of carbonaceous starting materials derived from natural materials, such as coal [25] and low-cost agricultural by-products [26–31] in an inert atmosphere (such as $N_2$ or Ar) and activation of the resulting char by $CO_2$ or $H_2O$ at high temperatures (600–1100 °C) [27] [32,33]. For the latter, carbonization and activation are carried out in the presence of $CO_2$ or $H_2O$ without an additional inert gas [34]. The one-step procedure was proposed to be more economically viable than the two-step procedure due to its lower activation temperature (500–900 °C). Recently, mesoporous templated-carbons have also been activated by using physical activation methods [35], and activation resulted in a significant increase in the microporosity. However, it is noteworthy that activation destroyed some mesoporous carbon rods and tubes, reducing the order degree of mesopores. Therefore, activation might influence the original porous structure and texture of the starting carbons in ways other than increasing the number of micropores, and further the application, which should be attracted attention. Moreover, to the best of our knowledge, there were no reports of the physical activation of macroporous diatomite-templated carbons, until now. In this case, it is quite interesting and practically significant to evaluate the influence of physical activation on the porosity of the diatomite-templated carbons and their application.

In the present work, the one-step and two-step activation methods were performed with $CO_2$ and $H_2O$ as the activation agent to enhance the porosity of diatomite-templated carbons, which were obtained using diatomite simultaneously as the template and the catalyst. The influence of activation on the porosity of diatomite-templated carbons was evaluated using $S_{BET}$, $V_p$, $V_m$, and the pore size distribution, and its effects on the adsorption capacity were assessed by MB adsorption. The structural and adsorptive properties of the resulting porous carbons were studied based on combined characterization methods, including scanning electron microscopy (SEM), transmission electron microscopy (TEM), and $N_2$ adsorption–desorption.

## 2. Materials and methods

### 2.1. Diatomite

Raw diatomite sample was obtained from Qingshanyuan Diatomite Co., Ltd. (Jilin provinces, China), and purified by a sedimentation method [10,11]. The dominant diatoms of the purified samples (for the chemical compositions, see Supplementary Data) were of the genus *Coscinodiscus* Ehrenberg (Centrales), which is disk-shaped and has a highly developed porous structure (Fig. 1a).

### 2.2. Preparation and activation of the diatomite-templated porous carbons

The porous carbon product was prepared as follows: diatomite and furfuryl alcohol were mixed in ceramic boats with a solid/liquid ratio of 1 g: 5 mL, and then stirred for 1.5 h at room temperature, followed by heating at 95 °C for 24 h. The mixture was further heated at 150 °C under vacuum conditions for 1 h to promote cross-linking; it was then transferred into a tubular oven and heated at 700 °C for 3 h under a $N_2$ atmosphere (99.999%) for complete carbonization. The resulting product was dissolved in a 40% HF solution for 12 h to remove the diatomite template (1 g solid in 20 mL aqueous HF solution). The derived carbon was denoted C/Dt.

Two-step activation method using $CO_2$ as the activation agent was performed in a tubular oven as follows: an approximately 1.0 g C/Dt sample was heated in a ceramic boat to 800 °C at a heating rate of 10 °C/min for 2 h (the optimized temperature and time selected from a series of preliminary experiments, see Supplementary Data, Fig. S1) under a $CO_2$ atmosphere with a gas flow rate of 100 $cm^3$/min. The final carbon product was denoted C/Dt-$CO_2$. A similar procedure was performed for two-step activation using $H_2O$ with a steam flow rate of 200 $cm^3$/min. The derived carbon was denoted C/Dt-$H_2O$.

One-step activation was carried out after cross-linking of diatomite and furfuryl alcohol. The resulting mixture (approximate 1.0 g) was placed in a tubular oven and subsequently heated to 800 °C at a heating rate of 10 °C/min for 2 h under a $CO_2$ atmosphere with the gas flow rate of 100 $cm^3$/min (or 200 $cm^3$/min for $H_2O$). The resulting product was dissolved in a 40% HF solution for 12 h to remove the diatomite template (1 g solid in 20 mL aqueous HF solution). The final carbon product was denoted C′/Dt-$CO_2$ (or C′/Dt-$H_2O$).

### 2.3. MB adsorption

In a typical run of MB ($C_{16}H_{18}ClN_3S_2{\cdot}3H_2O$; Molecule Weight: 373.9 g/mol; Tianjin Kermel Chemical Reagent Co. Ltd., China) adsorption kinetics test, 0.1 g carbon products was added to a 15 mL MB solution (concentration: 500 mg/L); then, the mixture was strongly shaken at a rate of 200 rpm in an oscillator to ensure complete mixing at room temperature. The contact time was in the range of 5–180 min. At timed intervals, the mixture was centrifuged, and the supernatant was used for the determination of the MB content, which was performed on a UV–vis spectroscopy at wavelength of 665 nm. The adsorption amount ($q_e$, mg MB/g carbon) was calculated using the following equation:

$$q_e = \frac{(C_0 - C_t)V}{M} \quad (1)$$

where $C_0$ and $C_t$ (mg/L) are the MB concentration in the reaction solution before and after adsorption, respectively; $V$ (L) is the solution volume; and $M$ (g) is the amount of the adsorbent, 0.1 g.

The adsorption isotherm is simulated using the Langmuir model and the linear form of the Langmuir model is given as:

$$\frac{C_e}{Q_e} = \frac{1}{k_L Q_m} + \frac{1}{Q_m} C_e \quad (2)$$

where $k_L$ (L/g) and $Q_m$ (mg/g) are the Langmuir constant and the monolayer adsorption capacity, respectively, and $C_e$ (mg/L) is the equilibrium concentration of the MB solution.

The affinity between adsorbent and adsorbate are evaluated based on the separation factor, $R_L$, determined from the Langmuir adsorption isotherm model [36,37]. $R_L$ is defined by the following equation:

$$R_L = \frac{1}{1 + k_L C_0} \quad (3)$$

where $C_0$ (mg/L) is the initial concentration of MB and $K_L$ (L/mg) is the Langmuir constant related to the energy of adsorption.

### 2.4. Characterization methods

SEM micrographs were obtained using a 5 kV FEI-Sirion 200 field emission scanning electron microscope. TEM images were obtained on a JEOL JEM-2100 electron microscope operating at an acceleration voltage of 200 kV. The specimens for TEM observation were prepared as follows: the sample was ultrasonically dispersed in ethanol for 5 min, and then a drop of the sample suspension was placed onto a carbon-coated copper grid. The grid was left to stand for 10 min before being transferred into the microscope.

The $N_2$ adsorption–desorption.isotherms were measured on a Micromeritics ASAP 2020 system (Micromeritics Co., Norcross, USA) at liquid nitrogen temperature. Before the measurement, the samples were outgassed at 150 °C for 12 h at the degas port and were then transferred to the analysis port to degas under a relative pressure of 0.01 for additional 6 h. $S_{BET}$ was calculated using the multiple-point Brunauer–Emmett–Teller (BET) method, and $V_p$ was evaluated from the $N_2$ uptake at a relative pressure of approximately 0.99. $V_m$ was estimated using the HK methods [38]. Micropore size distributions in the range of 0.35–2 nm were determined using non-local density functional theory (NLDFT) [39].

## 3. Results and discussion

### 3.1. SEM and TEM

The diatom shell of Dt possesses well-developed pores, and two types of macropores are exhibited in Fig. 1a. The macropores in the center of shells are not arrayed regularly, and their pore sizes are concentrated in the range of 300–800 nm (Fig. 1a); the edge macropores show an ordered array with pore size in the range of 100–250 nm (Fig. 1a insert). The C/Dt and Dt morphologies are highly comparable (See Supplementary Data, Fig. S2), indicating the replication of the carbon product from the diatomite template. The macroporous structure is composed of carbon pillars and tubes, and these pillars and tubes were derived from the central and edge macropores of diatomite shells, respectively (For the formation mechanisms, see our previous report [10]). After activation by $CO_2$ and $H_2O$ in the two-step method, both the tubular and pillared structures of the carbon products still remained, as revealed by SEM/TEM (Fig. 1b–g, herein, take C/Dt-$CO_2$ as an example). A SEM cross-section of a C/Dt-$CO_2$ particle (Fig. 1b) shows two complete carbon pillars, which are connected by the carbon film and are filled with carbon particles from the "*in situ*" carbonization of furfuryl alcohol [10,11], as confirmed by its TEM image (Fig. 1e). The carbon tubes derived from the replication of edge macropores of diatom shell exhibit an ordered arrangement, as observed in the planform (Fig. 1c) and cross-sectional views (Fig. 1d) of C/Dt-$CO_2$. These carbon tubes are completely hollow, as revealed by TEM (Fig. 1f), and show different macropore sizes for two openings of 150–200 nm and ~100 nm, respectively (Fig. 1c and d). In the walls of carbon tubes and pillars, there exist abundant

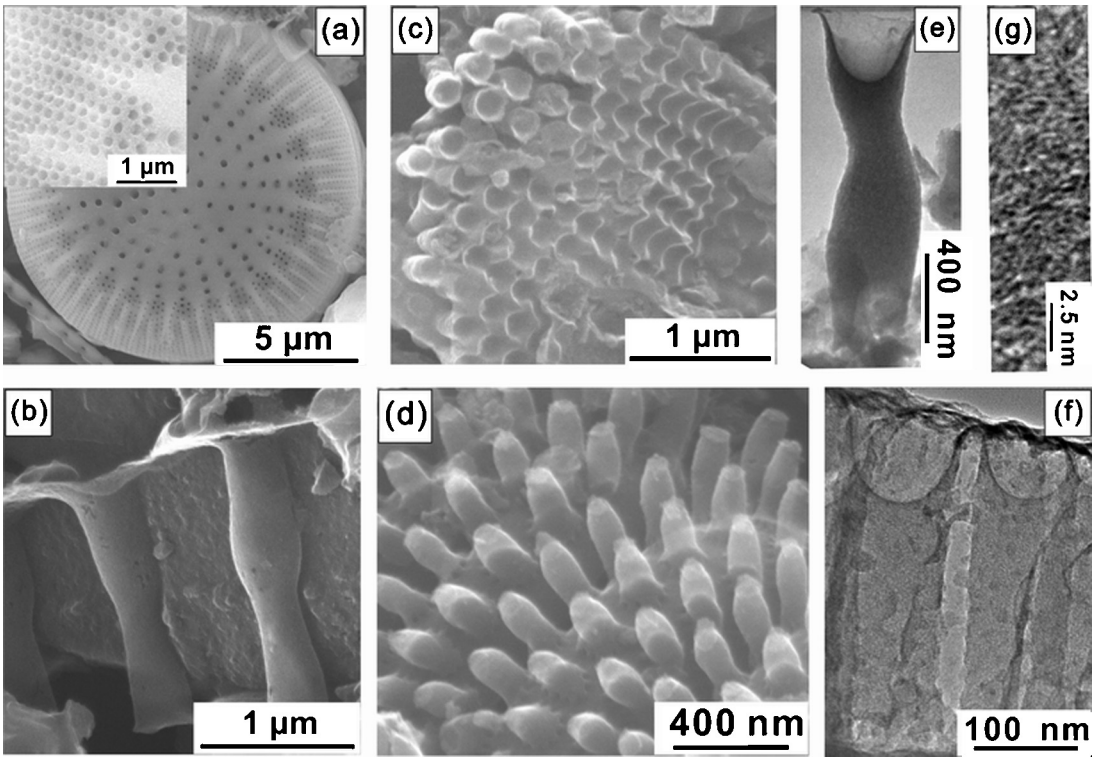


**Fig. 1.** SEM images of (a) diatom shell of Dt (insert: edge macropores of diatom shell), (b) carbon pillars C/Dt-$CO_2$, (c and d) carbon tubes of C/Dt-$CO_2$; TEM images of (e) carbon pillars of C/Dt-$CO_2$, (f) carbon tubes of C/Dt-$CO_2$, (g) micropores of C/Dt-$CO_2$.

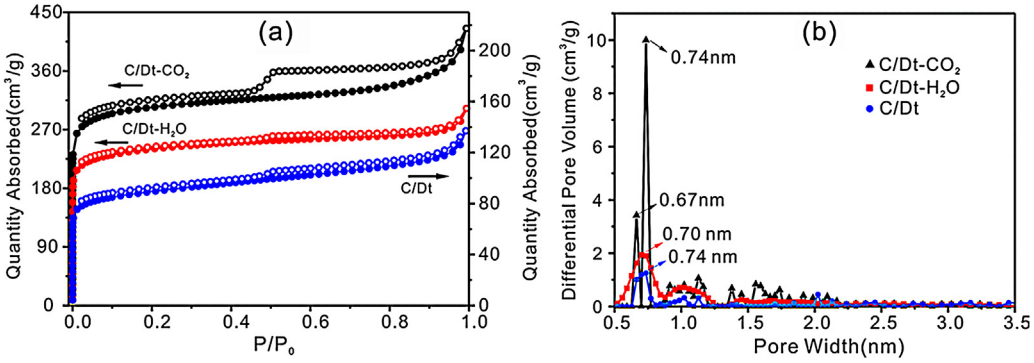


**Fig. 2.** (a) $N_2$ adsorption isotherms of diatomite-templated carbons before and after activation; (b) micropore size distributions of carbons.

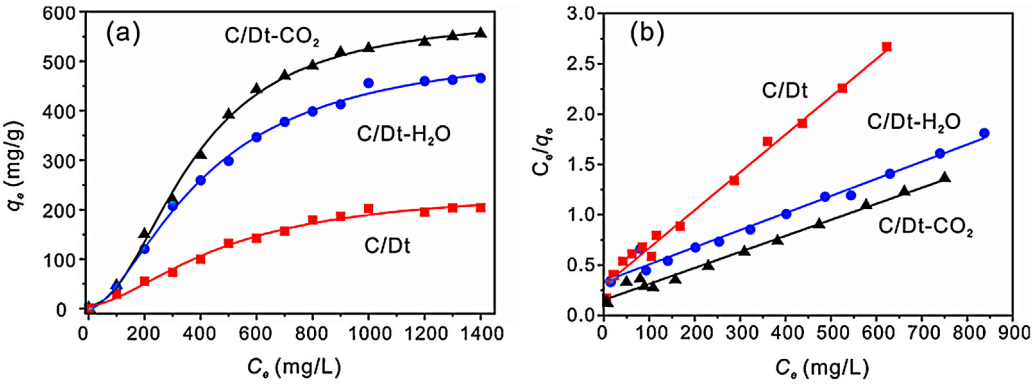


**Fig. 3.** (a) The MB adsorption isotherms of C/Dt, C/Dt-$CO_2$, and C/Dt-$H_2O$; (b) linear fitting plots based on Langmuir isotherm model for MB adsorption.

micropores, most of which are narrow slit-like with pore sizes smaller than 1 nm (Fig. 1g). These well-preserved carbon tubes, pillars, and their walls indicated that activation did not destroy the monolithic construction.

However, carbons obtained by the one-step activation method possess very few carbon pillars and tubes, as showed in Supplementary Data, Fig. S3. Abundant carbon plate fragments appear in the SEM images, and no pillared or tubular carbon structures are exhibited inside the field of view. This result indicated that one-step activation destroyed the macroporous structure and was not suited to enhancing the porosity of diatomite-templated carbons which should have an advantage in the macroporosity. The main reason proposed for the structural deconstruction was that after one-step activation an abundance of micropores existed in the walls of carbon tubes and pillars, decreasing the stability of the carbon texture. When the removal of diatomite templates, a lot of micropores formed in the carbon walls derived from the break of the carbon film [11], destroying the unstable carbon texture. In this case, it was not necessary to measure the properties of carbon products obtained by the one-step activation method, such as the pore parameters and the MB adsorption capacity, and these were ignored in this study. The activation method presented in the following text represents the two-step activation method.

### 3.2. $N_2$ adsorption

Before and after activation, the carbons exhibit type II adsorption isotherms (Fig. 2a). There are H3-type hysteresis loops between the adsorption and desorption isotherms for all carbons, reflecting the existence of micropores and mesopores. These typical H3 hysteresis loops imply that the micropores in the carbons were mainly slit-like [40,41], which was in good agreement with the TEM results, and were mainly attributed to the stacking of platy carbon microparticles [42]. The sharp increase in the $N_2$ adsorbed quantity near the relative pressure of 1.0 indicates the existence of macropores in all carbons, and these macropores were corresponded to the carbon tubes and pillars.

**Table 1**
Porous parameters of diatomite-templated carbons before and after activation.

| Samples | $S_{BET}$ ($m^2$/g) | $V_p$ ($cm^3$/g) | $V_m$ ($cm^3$/g) |
|---|---|---|---|
| C/Dt | 270 | 0.212 | 0.127 |
| C/Dt-$CO_2$ | 886 | 0.658 | 0.437 |
| C/Dt-$H_2O$ | 789 | 0.438 | 0.343 |

The $S_{BET}$, $V_p$, and $V_m$ values of C/Dt are 270 $m^2$/g, 0.212 $cm^3$/g, and 0.127 $cm^3$/g, respectively (Table 1). After activation, the porous parameters of the carbon products greatly increased and were 2–3 times larger than those of C/Dt. For example, the $S_{BET}$ values of C/Dt-$CO_2$ (886 $m^2$/g) and C/Dt-$H_2O$ (789 $m^2$/g) were, respectively, 2.9 and 3.3 times larger than that of C/Dt; and in particularly, the $V_m$ value increased to 0.437 $cm^3$/g after $CO_2$ activation, making it 3.4 times larger than that of C/Dt. The micropore rate, which was obtained from the ratio of $V_m$ to $V_p$, was enhanced from 59.9% to 66.4% and 78.3% after activation by $CO_2$ and $H_2O$, respectively. The high $V_p$ and micropore rate demonstrated that the pores "created" by $CO_2$ and $H_2O$ activation were mainly micropores. Moreover, the $S_{BET}$, $V_p$, and $V_m$ values of C/Dt-$CO_2$ are higher than those of C/Dt-$H_2O$, indicating that the activation effect on the porosity by $CO_2$ was better than by $H_2O$.

The micropore size distributions of C/Dt (Fig. 2b) show that one primary population appears at approximately 0.74 nm and that a secondary population appears at approximately 1.0 nm. These populations mainly correspond to the micropores generated by the structure-reconfiguration of the carbon film during the removal of the diatomite template [10,11]. After $CO_2$ activation, in

**Table 2**
Langmuir equation parameters for MB adsorption on various adsorbents.

| Model | Parameters | Adsorbents | | |
|---|---|---|---|---|
| | | C/Dt-$CO_2$ | C/Dt-$H_2O$ | C/Dt |
| Langmuir | $R^2$ | 0.9838 | 0.9765 | 0.9910 |
| | $K_L$ | 0.013 | 0.064 | 0.010 |
| | $Q_m$ (mg/g) | 505.1 | 476.2 | 250.0 |
| | $R_L$ | 0.35–0.88 | 0.10–0.61 | 0.066–0.50 |

addition to the populations at 0.74 and 1.0 nm, there appears a sharp population at 0.67 nm and some smaller populations at 1.2, 1.4, 1.6, and 1.7 nm (Fig. 2b), which were attributed to the newly formed micropores. Moreover, the volume of 0.74 nm micropores increased greatly after $CO_2$ activation, indicating that some "created" micropores possessed a pore size of 0.74 nm. Two wide populations, centered at 0.70 and 1.0 nm in the micropore size distribution of C/Dt-$H_2O$, had higher pore volumes than those of populations centered at 0.74 and 1.0 nm in the size distributions of C/Dt (Fig. 2b). The increased pore volumes of the two populations might be attributed to newly appeared micropores with pore sizes centered at approximately 0.70 and 1.0 nm. The differences in the micropore size distributions of the two carbon products derived from activation might be relevant to the activation mechanisms and properties, such as the size and reactivity, of two activation reagents; however, at this stage, it is still difficult to confirm the differences.

### 3.3. MB adsorption

The effects of activation on the adsorption capacity were evaluated by MB adsorption. Fig. 3a displays the MB adsorption isotherms for the carbons before and after activation, showing that the adsorption capacity initially increased with increasing MB concentration and then gradually reached a maximum at a high MB concentration. The Langmuir, Freundlich, and Redlich–Peterson isotherm models were used to fit the experimental data and quantitatively describe the adsorption data; the Langmuir model ($R^2 > 0.97$) correlated better than the Freundlich and Redlich–Peterson models (not showed). The $Q_m$ values obtained from the linear form of the Langmuir model (Eq. (2)) were 250.0 mg/g for C/Dt, 505.1 mg/g for C/Dt-$CO_2$, 476.2 mg/g for C/Dt-$H_2O$ (Table 2). These results show that C/Dt-$CO_2$ and C/Dt-$H_2O$ had much higher MB adsorption capacities than C/Dt, indicating that activation increased the MB adsorption capacity of the diatomite-templated carbon. The increased MB adsorption capacity was attributed to the newly appeared pores. Moreover, the fact that the MB adsorption capacity of C/Dt-$CO_2$ was higher than that of C/Dt-$H_2O$ implied the effect of $CO_2$ activation on the adsorption capacity was better than that of $H_2O$ activation.

$R_L$ values obtained by Eq. (3) were used to evaluate the affinity between MB and the diatomite-templated carbons before and after activation: $R_L > 1$, unfavorable adsorption; $R_L = 1$, linear adsorption; $0 < R_L < 1$, favorable adsorption; and $R_L \approx 0$, irreversible adsorption [37]. As showed in Table 2, the $R_L$ values corresponding to all carbons are in the range of 0–1, indicating the favorable MB uptake of these carbons.

## 4. Conclusions

Two-step and one-step activation methods using $CO_2$ or $H_2O$ as the activation agent were performed to enhance the porosity of diatomite-templated carbons. The results showed that two-step activation was better fitting than one-step activation during which the macroporous structure of diatomite-templated carbons was destroyed. The carbon products obtained by the two-step activation method not only retained the unique tubular and pillared macroporous structure of the original diatomite-templated carbon but also showed much higher surface areas and pore volumes, as well as larger MB adsorption capacity, than the original carbon.

After two-step activation by $CO_2$ or $H_2O$, an abundance of micropores appeared, resulting in a 2–3 times increase in the specific surface area and pore volume. Additionally, the micropore rate increased to 66.4% and 78.3% for the $CO_2$- and $H_2O$-activated carbons, respectively. The size distribution of the new-appearing micropores was centered at 0.67 and 0.74 nm for the $CO_2$-activated carbon, and 0.70 and 1.0 nm for the $H_2O$-activated carbon. The derived carbon products exhibited a higher MB adsorption capacity after activation; the maximum Langmuir adsorption capacity of MB on the $CO_2$-activated carbon was 505.1 mg/g, which was over 2 times larger than that of the original carbon, as well as larger than that of $H_2O$-activated carbons.

These fundamental results indicate that two-step activation by $CO_2$ or $H_2O$ can greatly enhance the porosity of diatomite-templated carbons and that $CO_2$ activation is more effective than $H_2O$ activation. This physical activation method is demonstrated to be promising for preparing hierarchically porous structural carbons with the high adsorption capacity.

## Acknowledgements

The financial supports from the National Natural Scientific Foundation of China (Grant Nos. 41202024 and 40872042) and National Key Technology Research and Development Program of the Ministry of Science and Technology of China (Grant No. 2013BAC01B02) are gratefully acknowledged. This is a contribution (No. IS1691) from GIGCAS.

## Appendix A. Supplementary data

Supplementary data associated with this article can be found, in the online version, at http://dx.doi.org/10.1016/j.apsusc.2013.06.067.

## References

[1] Z.H. Hu, M.P. Srinivasan, Y.M. Ni, Preparation of mesoporous high-surface-area activated carbon, Advanced Materials 12 (2000) 62–65.
[2] J. Lee, J. Kim, T. Hyeon, Recent progress in the synthesis of porous carbon materials, Advanced Materials 18 (2006) 2073–2094.
[3] C.D. Liang, Z.J. Li, S. Dai, Mesoporous carbon materials: synthesis and modification, Angewandte Chemie International Edition 47 (2008) 3696–3717.
[4] S. Alvarez, T. Valdes-Solis, A.B. Fuertes, Templated synthesis of nanosized mesoporous carbons, Materials Research Bulletin 43 (2008) 1898–1904.
[5] B. Sakintuna, Y. Yurum, Templated porous carbons: a review article, Industrial & Engineering Chemistry Research 44 (2005) 2893–2902.
[6] Z. Yang, Y. Xia, X. Sun, R. Mokaya, Preparation and hydrogen storage properties of zeolite-templated carbon materials nanocast via chemical vapor deposition: effect of the zeolite template and nitrogen doping, The Journal of Physical Chemistry B 110 (2006) 18424–18431.
[7] Z.X. Ma, T. Kyotani, A. Tomita, Preparation of a high surface area microporous carbon having the structural regularity of Y zeolite, Chemical Communications 236 (2000) 5–236, 6.
[8] T. Kyotani, T. Nagai, S. Inoue, A. Tomita, Formation of new type of porous carbon by carbonization in zeolite nanochannels, Chemistry of Materials 9 (1997) 609–615.
[9] C. Liang, Z. Li, S. Dai, Mesoporous carbon materials: synthesis and modification, Angewandte Chemie International Edition 120 (2008) 3754–3776.
[10] D. Liu, P. Yuan, D.Y. Tan, H.M. Liu, M.D. Fan, A.H. Yuan, J.X. Zhu, H.P. He, Effects of inherent/enhanced solid acidity and morphology of diatomite templates on the synthesis and porosity of hierarchically porous carbon, Langmuir 26 (2010) 18624–18627.
[11] D. Liu, P. Yuan, D.Y. Tan, H.M. Liu, T. Wang, M.D. Fan, J.X. Zhu, H.P. He, Facile preparation of hierarchically porous carbon using diatomite as both template and catalyst and methylene blue adsorption of carbon products, Journal of Colloid and Interface Science 388 (2012) 176–184.
[12] M. Perez-Cabero, V. Puchol, D. Beltran, P. Amoros, *Thalassiosira pseudonana* diatom as biotemplate to produce a macroporous ordered carbon-rich material, Carbon 46 (2008) 297–304.

[13] S.M. Holmes, B.E. Graniel-Garcia, P. Foran, P. Hill, E.P.L. Roberts, B.H. Sakakini, J.M. Newton, A novel porous carbon based on diatomaceous earth, Chemical Communications 266 (2006) 2–266, 3.
[14] P. Yuan, D. Yang, Z. Lin, H. He, X. Wen, L. Wang, F. Deng, Influences of pretreatment temperature on the surface silylation of diatomaceous amorphous silica with trimethylchlorosilane, Journal of Non-Crystalline Solids 352 (2006) 3762–3771.
[15] P. Yuan, D.Q. Wu, H.P. He, Z.Y. Lin, The hydroxyl species and acid sites on diatomite surface: a combined IR and Raman study, Applied Surface Science 227 (2004) 30–39.
[16] P. Yuan, D. Liu, M. Fan, D. Yang, R. Zhu, F. Ge, J.X. Zhu, H. He, Removal of hexavalent chromium [Cr(VI)] from aqueous solutions by the diatomite-supported/unsupported magnetite nanoparticles, Journal of Hazardous Materials 173 (2010) 614–621.
[17] E.K. Payne, N.L. Rosi, C. Xue, C.A. Mirkin, Sacrificial biological templates for the formation of nanostructured metallic microshells, Angewandte Chemie International Edition 44 (2005) 5064–5067.
[18] Y.J. Wang, Y. Tang, A.G. Dong, X.D. Wang, N. Ren, Z. Gao, Zeolitization of diatomite to prepare hierarchical porous zeolite materials through a vapor-phase transport process, Journal of Materials Chemistry 12 (2002) 1812–1818.
[19] M.A. Al-Ghouti, Y.S. Al-Degs, New adsorbents based on microemulsion modified diatomite and activated carbon for removing organic and inorganic pollutants from waste lubricants, Chemical Engineering Journal 173 (2011) 115–128.
[20] H. Hadjar, B. Hamdi, M. Jaber, J. Brendlé, Z. Kessaïssia, H. Balard, J.B. Donnet, Elaboration and characterisation of new mesoporous materials from diatomite and charcoal, Microporous Mesoporous Materials 107 (2008) 219–226.
[21] X. Cai, G.S. Zhu, W.W. Zhang, H.Y. Zhao, C. Wang, S.L. Qiu, Y. Wei, Diatom-templated synthesis of ordered meso/macroporous hierarchical materials, European Journal of Inorganic Chemistry 364 (2006) 1–364, 5.
[22] K.V. Kumar, S. Sivanesan, Equilibrium data, isotherm parameters and process design for partial and complete isotherm of methylene blue onto activated carbon, Journal of Hazardous Materials 134 (2006) 237–244.
[23] M. Rafatullah, O. Sulaiman, R. Hashim, A. Ahmad, Adsorption of methylene blue on low-cost adsorbents: a review, Journal of Hazardous Materials 177 (2010) 70–80.
[24] F. Rodriguez-Reinoso, M. Molina-Sabio, Activated carbons from lignocellulosic materials by chemical and/or physical activation: an overview, Carbon 30 (1992) 1111–1118.
[25] E.N. El Qada, S.J. Allen, G.A. Walker, Adsorption of basic dyes from aqueous solution onto activated carbons, Chemical Engineering Journal 135 (2008) 174–184.
[26] A.C. Lua, J. Guo, Activated carbon prepared from oil palm stone by one-step $CO_2$ activation for gaseous pollutant removal, Carbon 38 (2000) 1089–1097.
[27] A.R. Sanchez, A.A. Elguezabal, L.L.T. Saenz, $CO_2$ activation of char from *Quercus agrifolia* wood waste, Carbon 39 (2001) 1367–1377.
[28] T. Yang, A.C. Lua, Characteristics of activated carbons prepared from pistachio-nut shells by physical activation, Journal of Colloid and Interface Science 267 (2003) 408–417.
[29] I.A.W. Tan, B.H. Hameed, A.L. Ahmad, Equilibrium and kinetic studies on basic dye adsorption by oil palm fibre activated carbon, Chemical Engineering Journal 127 (2007) 111–119.
[30] P. Gonzalez-Garcia, T.A. Centeno, E. Urones-Garrote, D. Avila-Brande, L.C. Otero-Diaz, Microstructure and surface properties of lignocellulosic-based activated carbons, Applied Surface Science 265 (2013) 731–737.
[31] S. Erdogan, Y. Onal, C. Akmil-Basar, S. Bilmez-Erdemoglu, C. Sarici-Ozdemir, E. Koseoglu, G. Icduygu, Optimization of nickel adsorption from aqueous solution by using activated carbon prepared from waste apricot by chemical activation, Applied Surface Science 252 (2005) 1324–1331.
[32] S.H. Guo, J.H. Peng, W. Li, K.B. Yang, L.B. Zhang, S.M. Zhang, H.Y. Xia, Effects of $CO_2$ activation on porous structures of coconut shell-based activated carbons, Applied Surface Science 255 (2009) 8443–8449.
[33] J. Ganan, J.F. Gonzalez, C.M. Gonzalez-Garcia, A. Ramiro, E. Sabio, S. Roman, Carbon dioxide-activated carbons from almond tree pruning: preparation and characterization, Applied Surface Science 252 (2006) 5993–5998.
[34] K. Gergova, S. Eser, Effects of activation method on the pore structure of activated carbons from apricot stones, Carbon 34 (1996) 879–888.
[35] K. Xia, Q. Gao, C. Wu, S. Song, M. Ruan, Activation, characterization and hydrogen storage properties of the mesoporous carbon CMK-3, Carbon 45 (2007) 1989–1996.
[36] K.R. Hall, L.C. Eagleton, A. Acrivos, VermeuleT., Pore-solid-diffusion kinetics in fixed-bed adsorption under constant-pattern conditions, Industrial & Engineering Chemistry Research 5 (1966) 212–216.
[37] T.W. Weber, ChakravoRk, Pore and solid diffusion models for fixed-bed adsorbers, AIChE Journal 20 (1974) 228–238.
[38] G. Horvath, K. Kawazoe, Method for the calculation of effective pore-size distribution in molecular-sieve carbon, Journal of Chemical Engineering of Japan 16 (1983) 470–475.
[39] C.G. Sonwane, S.K. Bhatia, Characterization of pore size distributions of mesoporous materials from adsorption isotherms, The Journal of Physical Chemistry B 104 (2000) 9099–9110.
[40] P.M. Barata-Rodrigues, T.J. Mays, G.D. Moggridge, Structured carbon adsorbents from clay, zeolite and mesoporous aluminosilicate templates, Carbon 41 (2003) 2231–2246.
[41] K. Sing, R. Williams, Physisorption hysteresis loops and the characterization of nanoporous materials, Adsorption Science and Technology 22 (2004) 773–782.
[42] K.S.W. Sing, R.T. Williams, Review, The use of molecular probes for the characterization of nanoporous adsorbents, Particle & Particle Systems Characterization 21 (2004) 71–79.